Microwave Tomography for Food Contamination Monitoring

Microwave Tomography for Food Contamination Monitoring

M. Ricci *, L. Crocco † F. Vipiana *
*Dept. of Electronics and Telecommunications, Politecnico di Torino, Torino, Italy,
email: marco.ricci, francesca.vipiana@polito.it
†CNR-IREA, Consiglio Nazionale delle Ricerche, Napoli, Italy,
email: crocco.l@irea.cnr.it

***Abstract*—The security of packaged food needs to be guaranteed to safeguard customers health. A raise of complaints of physical contaminations into food products pushes for the development of additional monitoring techniques to prevent any kind of hazards, but also to protect brands from customers trust loss. In this work, a prototype working at microwave frequencies is assessed and tested in a significant environment. It exploits the dielectric contrast between contaminants and food content, and it is it is mainly focused on two classes of intrusions matters, i.e. plastic and glass fragments of few mm size, that have limited detection by the existing in-line technologies, such as X-rays systems. The measurements and the resulting 3-D image reconstructions are encouraging and allow to aim at the development of an industrial prototype, monitoring packaged food in real-time along a production line.**

***Index Terms*—microwave imaging, non-invasive diagnostics, food inspection, food security, food safety**

I. Introduction

Food contamination monitoring is increasingly calling for the development of new technologies to increase the safety of food products. As a matter of fact, the employed systems, in particular metal detectors (MD) and X-rays (XRI), fail in the detection of some class of contaminants, such as fragments of glass of low-density plastics. This is proven by the constant raise of food recalls due to physical contamination, plastic primarily, mainly due to customers complaints [1].

The potential risks of contaminated products are multiple: first, the hazard for consumers in case of accidental ingestion, potentially leading to severe injuries; further, the economic consequences for industries due to large recall expenses and also the customers loss of trust in affected brands.

During the last years, a growing interest has been shown towards Microwave Imaging (MWI) [2] for food monitoring [3]. Differently from ohter inspection techniques, MWI is based on the analysis of the dielectric constrast between the intrusions and the food content. An industrial implementation has been developed as well [4], employed for monitoring fluids along pipes before packaging, which is actually one of the most hazardous step in the production chain. Indeed, the mechanized process can fail and break the food containers or seals, resulting in a potential contamination.

J. Tobon et al. presented in [5] a MWI system implementation at industrial level by using one antennas pair placed on the two side of the packaging conveyor belt. Data metrics showed that the system is able to detect the presence of contaminants, but collected signals were not sufficient for a 3-D image reconstruction. An upgrade of such implementation has been preliminarily shown in [6], where a sytem of six antennas is built to generate a 3-D image of the object to analyze.

Here, results obtained with measurements of an effective multi-view prototype are reported and confirm the initial findings obtained with synthetic data; its implementation required ad-hoc hardware components in order to deal with a multiple antennas system measured with a two-port Vector Network Analyzer (VNA): it consists in a switching matrix to pilot

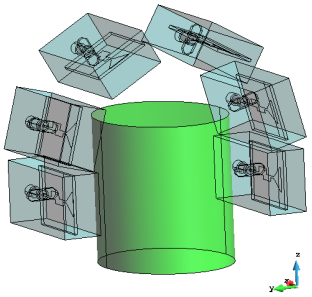

Fig. 1. Antennas array position with respect to the object under analysis.

Fig. 2. Switching matrix connected to the antennas array and the Vector Network Analyzer.

the transmission of the full antennas array, and further a 3-D printed antennas support to replicate the positions selected in its numerical assessment.

II. MWI SYSTEM LAYOUT

The objective of the presented architecture is to obtain a 3-D image of the volume of interest, by adopting an arch-shaped antennas array, studied to fit along a conveyor belt without interrupting the production process. Its implementation is shown in Figure 1; the antennas are printed monopoles, and their number and position with respect to the target have been set by a rigorous procedure based on the singular value decomposition (SVD) of the discretized scattering operator proposed in [7] and already used for the realization of MWI systems for medical applications [8], [9] .

A. Theoretical background

MWI is an inverse scattering, ill-posed and non-linear problem. However, due to the low contrast in terms of volume and dielectric features between the intrusion and the surrounding food content, the distorted Born approximation can be applied to linearize it. Moreover the imaging task can be carried out under a differential configuration. In particular, the differential scattering matrix is obtained by measuring a "clean" target (without any contamination) and subtracting the scattering matrix of a target with an intrusion. Under these assumptions the imaging problem can be formulated as:

$$\Delta S(r_p, r_q) \approx \mathcal{L}(\Delta\chi) \tag{1}$$

where ΔS is the measured differential scattering matrix, r_p and r_q represents all the possible antenna pairs and $\mathcal{L}(\Delta\chi)$ denotes the linear scattering operator depending on the dielectric contrast only. As this problem is ill-posed, a regularization method has to be applied for its reliable solution. Here, the truncated singular value decomposition (TSVD) is exploited to compute a stable approximation of the inverse of the operator $\mathcal{L}$. Accordingly, one gets the explicit inversion formula:

$$\Delta\chi = \sum_{n=1}^{T} \frac{1}{\sigma_n} \langle U_n, \Delta S \rangle V_n \tag{2}$$

where $\Delta\chi$ is the reconstructed dielectric contrast and σ_n, U_n and V_n are obtained by the SVD and represent the singular values, left and right singular functions respectively of the discretized operator, which are then truncated at T to regularize the problem and allowing to build the 3-D image [10].

Fig. 3. The two considered contaminants, circled in red: on the left, a 2 mm radius PTFE sphere, on the right a glass splinter of approximately same dimensions.

Fig. 4. The two considered intrusions with respect to a reference coin to better realize their small dimensions.

B. Prototype design

The actual implementation of the prototype has been obtained by using the mentioned monopole antennas, whose positions are assured through a 3-D printed support, used to replicate the exact same placement as for the numerical assessment. The availability of a two-port VNA [11] forced the development of a switching matrix, shown in Figure 2; it consists in electro-mechanical switches, connecting the antennas to be measured to the VNA allowing the selected couple to be measured. It is piloted through the same software used to drive the VNA, and all the semi-rigid coaxial cables have the same length. As a first assessment, the measurements were performed with hazelnut-cocoa cream plastic jars, with an elliptical base of radii 3.3 cm and 4.2 cm and height of around 7.5 cm, in which samples of intrusion have been placed. Actually, after measuring the dielectric constant of such product, and considering the composition of chocolate creams, we noticed that it was convenient to replace it with safflower oil. From a dielectric point of view, the two products are almost equal: measured with a probe, the dielectric constant for the chocolate cream at 10 GHz is 3, while it is 2.86 with the considered oil. The conductivity is 0.23 Sm^{-1} for the cream and 0.21 Sm^{-1} for the oil. But from a practical point of view, safflower oil is easier to handle, in particular because of its transparency: indeed, the position of the inserted contamination can be evaluated more easily, to better understand if the imaging result could be considered satisfactory (Figure 3).

The two considered contaminants, shown in Figure 4 are respectively a teflon sphere, whose radius is 2 mm, and a glass splinter whose dimensions are almost the same. They are both hanging from a fishing wire, to better control their position, and surrounded by a really thin plastic envelope. The numerically computed operator and the corresponding measurements are taken at a frequency of 10 GHz, as a trade-off between penetration depth and resolution. The dielectric contrast is respectively $\Delta\chi_{plastic} = 1.117$ and $\Delta\chi_{glass} = 1.64$, which are considerably low values. The resolution can be considered as $\lambda/4$, which in the considered medium is 1.77

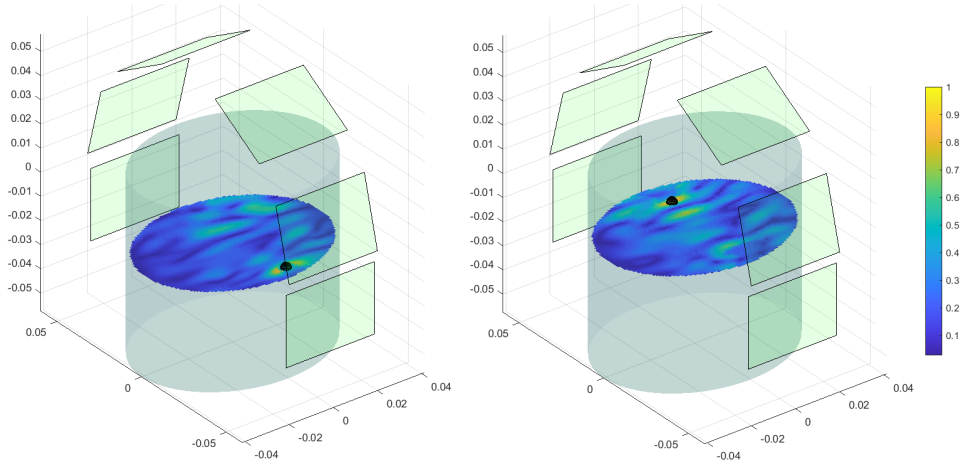

Fig. 5. Planar cut on the plane of the expected intrusion position, denoted as a black sphere. The antennas relative positions are represented through the transparent rectangles All lengths are in meters

mm, suitable for the dimensions of the considered intrusion. The measurement time is conditioned by the slowest device in the prototype, that is the switching matrix piloting the antennas in this case: this results in a total measuring time which is approximately 4 seconds. The scattering operator $\mathcal{L}$ is numerically computed with a in-house developed Finite Element Method solver [12].

III. Measurements reconstruction results

The 6×6 measured scattering matrices with the contaminant in the jar were differentiated from a measurement of the jar filled with oil only. Thanks to the Born-approximation, this difference can be considered due to the contamination solely. The reconstruction images are shown in Figure 5. They are enhanced thanks to an ad-hoc algorithm studied to balance the illumination of the target, due to the non-uniform fields radiated by the antennas. The expected position is represented by the black sphere, and the reconstructions are shown for the planar cut at the height where the contaminant positions have been estimated. The values are normalized for the whole volume; it is evident in both reconstructions, that high values are close to the expected positions, which means that the intrusions are correctly identified. A slight elongation along the axis passing through the gallery-shaped array can be noticed, and it it due to a lack of resolution along that direction.

IV. Conclusion and perspectives

The assessed scenario is valid for a static measurement in a controlled but significant environment. The reconstruction results are promising, even if there is room for improvement; one of the foreseen activities will be to exploit multiple frequencies for the tomographic reconstruction to further improve the reconstructions capabilities of the system. Finally, a validation with imaging of the object in motion along a production line prototype will validate the technology to a greater extent, but also it would enhance the imaging results by getting resolution along the motion axis. An extension of the VNA to a six-port device [11], triggered by a photocell detecting the passage of the object to analyze, will be a viable solution to allow a fast measurement, compatible with the conveyor belt speed.

Acknowledgment

This work was supported by the Italian Ministry of University and Research under the PRIN project “BEST-Food, Broadband Electromagnetic Sensing Technologies for Food Quality and Security Assessment.”

References

[1] The Rapid Alert System for Food and Feed, https://ec.europa.eu/food/sites/food/files/safety/docs/rasff_annual_report_2018.pdf

[2] Pastorino, M.. (2010). Microwave Imaging. Microwave Imaging. 10.1002/9780470602492.

[3] J. LoVetri et al., ”Innovations in Electromagnetic Imaging Technology: The Stored-Grain-Monitoring Case,” in IEEE Antennas and Propagation Magazine, vol. 62, no. 5, pp. 33-42, Oct. 2020, doi: 10.1109/MAP.2020.3003206.

[4] http://www.foodradar.com/

[5] J. A. Tobon Vasquez et al., ”Noninvasive Inline Food Inspection via Microwave Imaging Technology: An Application Example in the Food Industry,” in IEEE Antennas and Propagation Magazine, vol. 62, no. 5, pp. 18-32, Oct. 2020, doi: 10.1109/MAP.2020.3012898.

[6] M. Ricci, L. Crocco and F. Vipiana, ”Microwave Imaging Device for In-Line Food Inspection,” 2020 14th European Conference on Antennas and Propagation (EuCAP), Copenhagen, Denmark, 2020, pp. 1-4, doi: 10.23919/EuCAP48036.2020.9135775.

[7] Scapaticci, Rosa et al. “Design and Numerical Characterization of a Low-Complexity Microwave Device for Brain Stroke Monitoring.” IEEE Transactions on Antennas and Propagation 66 (2018): 7328-7338.

[8] J.A. Tobon et al., “Design and experimental assessmentof a 2D microwave imaging system for brain stroke monitoring,”Int. J.Antennas Propag., no. Article ID 8065036, p. 12 pages, 2019.

[9] J. A. Tobon Vasquez et al., “A Prototype Microwave System for 3D Brain Stroke Imaging”, SENSORS, Special Issue on Microwave Sensing and Imaging, 2020, 20, 2607 [DOI: 10.3390/s20092607].

[10] M. Bertero and P.Boccacci, Introduction to Inverse Problems in Imaging, Bristol, U.K.: Inst. Phys., 1998.

[11] Keysight Technologies, “M980xA Series PXIe Vector Network Analyzer,” Data Sheet, 2020.

[12] E. A. Attardo, A. Borsic, G. Vecchi and P. M. Meaney, ”Whole-System Electromagnetic Modeling for Microwave Tomography,” in IEEE Antennas and Wireless Propagation Letters, vol. 11, pp. 1618-1621, 2012.